Spectral Sidelobe Suppression of Nonuniform Pulse Repetition Frequency Waveforms in Strong Clutter

Sandun Kodituwakku, Van Khanh Nguyen, Mike D. Turley
National Security and ISR Division
Defence Science and Technology
Edinburgh, SA 5111, Australia.

***Abstract*—Standard spectral analysis of nonuniform sampled signals generates undesirable sidelobe levels and cannot be controlled via a window function as in the case of uniform sampled signals. We analyse two periodogram based techniques and four interpolation based techniques, and find that the iterative adaptive periodogram and the weighted bandlimited interpolation techniques are capable of achieving desired sidelobe levels. The weighted bandlimited interpolation is computationally less demanding and generates a spectrum similar to the uniform sampled signals, hence has advantages over the other techniques considered.**

I. Introduction

Nonuniform sampling of data naturally occurs or has advantages in a number of fields including astronomy, biomedical signal processing, and radar signal processing. Some of these applications are as follows: In astronomy, observations are often recorded in uneven periods in long time scales due to imperfect atmospheric conditions, and spectral analysis of such unevenly spaced time series data is often discussed [1]. In cardiac signal processing, heart beats are naturally occurring nonuniform sampling events used for heart rate variability analysis, which provides vital information of subject's health [2]. In radar waveforms, nonuniform pulse repetition provides a number of advantages including detecting targets with blind velocities [3].

In this paper, the focus is on spectral analysis of nonuniform pulse repetition frequency (PRF) radar waveforms. Doppler processing which involves spectral analysis of slow-time (inter-pulse) samples is a core step in radar signal processing to isolate clutter and detect targets based on their motion. With nonuniform PRF waveforms, Doppler processing becomes complicated by the fact that slow-time sample points are unevenly distributed. A standard Fourier based spectral analysis can still be applied with nonuniform samples, but it does not provide sufficient sidelobe suppression as will be demonstrated in Section II-A. Usually with a significant level of clutter present in radar returns, a sidelobe suppression of 60 dB or more may be required to detect targets of interest. In this paper, we analyse a number of techniques for the spectral analysis of nonuniform sampled signals, and evaluate them in terms of their sidelobe performance, complexity, and limitations.

Lomb-Scargle Periodogram [1], [4] which uses a least squares approach does not produce sufficiently low sidelobe levels in nonuniform sampled signals as we shall see in Section II-B. An adaptive technique, called iterative adaptive periodogram [5], is capable of achieving good sidelobes but is computationally more complex. It is iterative and each iteration requires a large matrix inversion. When spread Doppler such as clutter returns are present in the received signal, it is slow to converge, which makes this technique less attractive for real-time applications. Hence, our aim is to find an interpolation based technique which would resample nonuniform sampled signal into a uniform grid, and thereafter allows a standard spectral estimation technique developed for uniform sampled data to be applied.

In this paper, we analysed four interpolation techniques for spectral estimation of nonuniform PRF radar returns. Cubic spline interpolation is a commonly used interpolation technique for generating a piecewise smooth continuous-time signal based on cubic polynomial fitting [6]. However, it does not preserve the frequency characteristics of the underlying signal. Sinc kernel based interpolation is a perfect reconstruction of a bandlimited signal [7], however this result is only valid for a uniformly sampled signal. We show that cubic spline and sinc interpolation techniques fail to achieve desired sidelobe levels in the nonuniform case. A generalisation of the sinc interpolation to nonuniform samples is known as the Lagrange interpolation [8]. Even though desired sidelobe levels can be achieved using this technique, significant oscillations are observed in the resampled signal at the edges of the sampling interval (known as Runge's phenomenon) due to high degree polynomial based reconstruction. Hence, up to 50% of sample points may need to be discarded which will lead to signal to noise ratio (SNR) loss and reduced Doppler resolution.

We propose a weighted bandlimited interpolation method [9], [10] as a desirable interpolation technique for nonuniform PRF Doppler processing. In this technique sinc interpolation kernel is still used, but appropriately weighted according to nonuniform sampling intervals. Even though it requires computation of a weighting matrix, all the weights can be precomputed given that sampling times are known, and needs to be done only once. The weights are only dependent on sampling times and not on the received signal, hence it is still a linear non-adaptive interpolating filter and computationally less complex. We show that desirable sidelobe levels can be achieved by the weighted bandlimited interpolation for nonuniform PRF radar waveforms, producing similar performance to the uniform

sampling case. A limitation of the proposed techniques is also discussed for the Doppler aliased targets.

Section II formulates the problem of unconstrained spectral sidelobes in nonuniform PRF radar waveforms, and introduces Lomb-Scargle and iterative adaptive periodogram techniques. In Section III, we discuss four interpolation techniques mentioned previously. In Section IV, interpolation techniques are compared, and then the performance of the proposed techniques in detecting targets in clutter is analysed.

II. Preliminary

A. Nonuniform DFT

The discrete Fourier transform (DFT) of a discrete signal $s(t_n)$ sampled at $n = 1, \ldots, N$ is given by

$$S(f) = \sum_{n=1}^{N} s(t_n) e^{-j2\pi f t_n}. \tag{1}$$

This formula is applicable regardless of whether $s(\cdot)$ is sampled uniformly or nonuniformly. For a time-limited signal, the summation in (1) usually results in undesirable sidelobes in $S(f)$, thus a window function is usually applied to control the sidelobe levels. The choice of the window $w(\cdot)$ determined by the clutter power level achieves required sidelobe suppression for the conventional uniformly sampled signals. The corresponding spectrum is given by

$$S_w(f) = \sum_{n=1}^{N} s(t_n) w(t_n) e^{-j2\pi f t_n}. \tag{2}$$

Even though $S_w(f)$ can achieve satisfactory sidelobe levels in the uniformly sampled case (uniform sampling is defined as $t_n = nT$ where T is the uniform sampling period), for the nonuniform sampled case it still fails to achieve the desired sidelobe suppression. This is demonstrated in Figure 1. A complex sinusoid at 57.8 Hz is uniformly sampled with $T = 3.1$ ms. In the context of radar, the complex sinusoid model represents a radar return of a non-fluctuating target sampled in slow-time domain with PRF = 320 Hz. Blackman window is used for $w(\cdot)$ which gives -58 dB of sidelobe level when sampled uniformly. The same signal is sampled nonuniformly at $t_n = nT + \Delta_n$. Δ_n is a uniform random variable in $[-\kappa T, \kappa T]$. The constant $\kappa \in (0, 0.5)$ controls the randomness of the sampling points. This creates a set of random sampling points $t_n < t_{n+1}\ \forall n$, with an average sampling interval T. The nonuniform samples corresponds to slow-time signal from a radar system employing a nonuniform PRF radar waveform. In this example we set $\kappa = 0.05$. Even with this modest 5% variation of sampling times, the highest sidelobe has gone up to -42 dB. Thus, even the slightest changes in the sampling times will significantly affect the spectral estimation when DFT is computed directly from nonuniform samples.

Note that we compute $S_w(f)$ using the definition in (2), and any fast algorithm to compute $S_w(f)$ such as nonuniform fast Fourier transform (NUFFT) [11], though computationally more efficient, will give similar or slightly degraded spectral estimation.

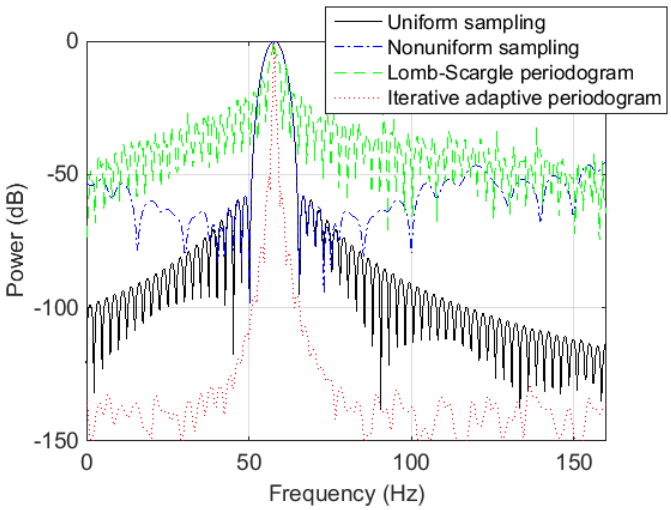

Fig. 1. DFT based spectral estimation of nonuniform sampled data with Blackman window compared with two periodogram based spectral estimations.

B. Lomb-Scargle Periodogram

The least squares periodogram, also known as Lomb-Scargle periodogram [1], [4], can be used to compute the spectrum based on the least squares fit of sinusoids to the nonuniform sampled signal. The spectral power estimated by this method is given by

$$P_{LS}(f) = \frac{1}{2\sigma^2} \frac{\left[\sum_{n=1}^{N} (s(t_n) - \bar{s}) e^{-j2\pi f(t_n - \tau)}\right]^2}{\sum_{n=1}^{N} e^{-j4\pi f(t_n - \tau)}} \tag{3}$$

where

$$\tau = \frac{1}{4\pi f} \arctan\left[\frac{\sum_{n=1}^{N} \sin(4\pi f t_n)}{\sum_{n=1}^{N} \cos(4\pi f t_n)}\right], \tag{4}$$

and $\bar{s}$ and σ^2 are mean and variance of $s(t_n)$, respectively. Note that Lomb-Scargle periodogram has been originally defined for real data, but is modified here for complex IQ data. Figure 1 shows Lomb-Scargle periodogram for the same nonuniform sampled signal as described in Section II-A. Its performance is worse than windowed DFT, but can be improved by applying a window to it.

C. Iterative Adaptive Periodogram

An iterative and adaptive spectral estimation technique is proposed by Stoica et al. in [5]. In this method, a weighted least-squares spectrum is estimated iteratively. In each iteration weighting coefficients are computed based on the previous spectral estimation. It is data dependant, hence an adaptive technique. Let f_k, $k = 1 \ldots K$, be the frequency points where the spectrum is computed. The complex sinusoid at f_k sampled at t_n is given by $\mathbf{a_k} = [\exp(j2\pi f_k t_1), \cdots, \exp(j2\pi f_k t_n)]^T$ as a column vector. Then, the basis of interest $\mathbf{A}$ is given by

$$\mathbf{A} = \left[\mathbf{a_1} \cdots \mathbf{a_K}\right]. \tag{5}$$

The vector of the received signal $s(t_n)$ is denoted by $\mathbf{s}$. The spectral estimation of $\mathbf{s}$ in the i^{th} iteration, $\mathbf{S}^i = [S_k^i]^T$, is given by

$$\mathbf{S}^i = [\mathbf{A}^H(\mathbf{R}^{i-1})^{-1}\mathbf{A}]^{-1}[\mathbf{A}^H(\mathbf{R}^{i-1})^{-1}\mathbf{s}], \tag{6}$$

where $\mathbf{R}^{i-1}$ is the weighting matrix computed from the previous iteration

$$\mathbf{R}^i = \mathbf{A}\,\mathrm{diag}(|S_k^i|^2)\,\mathbf{A}^H. \tag{7}$$

The weighting matrix is set to an identity matrix, i.e. $\mathbf{R}^0 = \mathbf{I}_N$, for the first iteration. The algorithm is terminated when $||\mathbf{S}^{i+1} - \mathbf{S}^i||_2 < \epsilon$ for a chosen positive small number ϵ.

The spectrum estimated using this method is shown in Figure 1. It achieves by far superior results to Lomb-Scargle periodogram or direct DFT based approach, and achieves a good isolation of the signal with a narrow mainlobe. Note that a window function is not required for the iterative adaptive periodogram as opposed to DFT based methods where a Blackman window was applied. Thus, the sidelobe structure is different to a typical window based method.

III. Interpolation Methods

Even though the iterative adaptive periodogram produces Doppler spectra with good sidelobe characteristics, its high complexity has implications on real-time applications. The weighting matrix $\mathbf{R}^i$ is a $N \times N$ matrix which needs to be inverted at each iteration. For radar systems employing a large number of pulses per coherent processing interval (CPI) this matrix becomes quite large, and such inversions could be highly time consuming and may not be feasible in real-time applications. On the other hand, FFT based computations are more attractive where optimised hardware implementations exist. Thus, we explore a number of techniques based on interpolation which resamples the signal into a uniform grid, and then applying DFT for spectral estimation with the focus on achieving desired sidelobe levels. Another advantage of interpolation based techniques is any desired non-parametric or parametric spectral estimation technique such as ARMA or MUSIC can be applied to the interpolated signal. For the simplicity, DFT is applied here for the spectral estimation of the resampled signal.

A review of few interpolation methods for nonuniform spectral analysis is presented in [12], where a number of kernel based and nearest neighbour interpolation techniques were discussed. The results shown in Figure 6 of [12] indicates sinc kernel based technique achieves superior results to Gaussian, Laplacian, or rectangular kernel based methods. In this paper, we also analyse the sinc kernel based method, but additionally introduce three other interpolation techniques, and analyse their performances in the context of nonuniform PRF radar Doppler processing.

A. Sinc Interpolation

Sinc interpolation (or Whittaker–Shannon interpolation) is a bandlimited interpolation technique and is derived from the famous sampling theory by Shannon [7], which states a bandlimited signal can be fully recovered from its samples given sampling frequency is at least twice the maximum frequency present in the signal. Sinc interpolation for a finite number of samples can be given as

$$s_S(t) = \sum_{n=1}^{N} s(t_n)\,\mathrm{sinc}\left(\frac{\pi(t-t_n)}{T}\right), \tag{8}$$

where sinc function is defined as $\mathrm{sinc}(x) = \sin(x)/x$, and T is the sampling period. Sinc interpolation is a perfect reconstruction for a uniformly sampled bandlimited signal, but two main issues arise for the problem addressed here: 1) T is the uniform sampling period and for the case of nonuniform sampling T needs to be approximated by the mean sampling interval; 2) perfect reconstruction is only possible with infinite number of samples, thus for a finite number of samples a truncation error occurs [13].

B. Cubic Spline Interpolation

Cubic spline interpolation is a piecewise polynomial interpolation technique. Cubic polynomials can be fitted to each adjacent pair of points $s(t_n)$ and $s(t_{n+1})$, $n = 1, \ldots, N-1$ to generate the interpolated signal $s_C(t)$ which can then be regularly sampled [6]. $s_C(t)$ for the interval $[t_n, t_{n+1}]$ is given by

$$s_{C,n}(t) = a_n + b_n t + c_n t^2 + d_n t^3, t \in [t_n, t_{n+1}] \tag{9}$$

where polynomial in each of the interval passes through the known end points, i.e. $s_{C,n}(t_n) = s(t_n)$ and $s_{C,n}(t_{n+1}) = s(t_{n+1})$. Also, polynomials in adjacent intervals agree in slope and curvature at the end points, i.e. $s_{C,n}^{'}(t_{n+1}) = s_{C,n+1}^{'}(t_{n+1})$ and $s_{C,n}^{''}(t_{n+1}) = s_{C,n+1}^{''}(t_{n+1})$. Above criteria with the boundary conditions $s_{C,1}^{''}(t_1) = s_{C,N-1}^{''}(t_n) = 0$ are sufficient to uniquely determine all the coefficients of $s_{C,n}(t)$ for each of the interval, thus a smoothed interpolated signal $s_C(t)$ can be formed piecewise. Note that $s_C^{'}(\cdot)$ and $s_C^{''}(\cdot)$ refer to first and second derivatives of $s_C(\cdot)$, respectively. Here, the interpolation is purely based on smoothing in the time domain, therefore spectral characteristics could be significantly different from that of the original signal.

C. Lagrange Interpolation

Lagrange interpolation is a single polynomial bandlimited interpolation technique [8]. For N sample points, the Lagrange interpolation polynomial of order $N-1$ is given by

$$s_L(t) = \sum_{n=1}^{N} s(t_n) P_n(t) \tag{10}$$

where

$$P_n(t) = \prod_{m=1}^{N} \frac{t - t_m}{t_n - t_m} \quad m \neq n. \tag{11}$$

Lagrange polynomial is the lowest degree polynomial that passes through all the known data points $(t_n, s(t_n))$. Lagrange interpolation is a generalisation of the sinc interpolation for nonuniform samples, and for the case of uniform sampling

it reduces to the sinc interpolation. However, a significant drawback of the Lagrange interpolation is that it generates very high oscillations at end sample points, which is known as the Runge's phenomenon. Thus, the interpolated signal diverges from the true signal at those points [14]. In order to overcome this problem, a percentage of samples at each end of the interpolated signal needs to be discarded.

D. Weighted Bandlimited Interpolation

Weighted bandlimited interpolation [9], [10] uses weighted sinc functions for the interpolation. The weights are calculated according to the nonuniform sampling points to compensate for variable intervals between samples. The interpolation formula is given by

$$s_{WB}(t) = \sum_{n=1}^{N} s(t_n) \left[\sum_{m=1}^{N} w_{mn} \operatorname{sinc}(\pi B(t - t_m)) \right] \quad (12)$$

where w_{mn} is the (m, n) element of the weighting matrix $\mathbf{W}$ given by

$$\mathbf{W} = \begin{bmatrix} \operatorname{sinc}(\pi B(t_1 - t_1)) & \cdots & \operatorname{sinc}(\pi B(t_N - t_1)) \\ \vdots & \ddots & \vdots \\ \operatorname{sinc}(\pi B(t_1 - t_N)) & \cdots & \operatorname{sinc}(\pi B(t_N - t_N)) \end{bmatrix}^{-1}. \quad (13)$$

B is the bandwidth of the signals of interest, and needs to be specified to satisfy the condition $B < 1/T$. Note that unlike in the iterative adaptive periodogram, $\mathbf{W}$ needs to computed only once. More so, since $\mathbf{W}$ is independent of the received signal and only dependant on nonuniform sampling times it can be precomputed, given that sampling times are predetermined.

IV. Results

A. Interpolation techniques comparison

We compare the performance of four interpolation techniques described in Section III. The simulation parameters are the same as in Section II-A, except $\kappa = 0.3$. The high κ gives highly randomised sampling points where variance in the sampling interval is 0.7 $(\text{ms})^2$, as opposed to zero variance in the uniform sampling case. DFT with Blackman window is applied after interpolation for the spectral estimation. Results are presented in Figure 2. Sinc interpolation which would give a perfect signal reconstruction for the uniform sampling case fails completely in the nonuniform case with highest sidelobes reaching -26 dB. Spline interpolation also has a high leakage of energy at the distant frequencies. In the case of Lagrange interpolation, 48% of the samples at the ends had to be removed due to high oscillations increasing the 3 dB mainlobe width from 4.1 Hz to 8.0 Hz. This corresponds to reduced Doppler resolution. On the other hand, the weighted bandlimited interpolation achieves -58 dB sidelobe levels as in the case of uniform sampling without any loss of resolution. It has a similar sidelobe structure and similar performance to DFT of uniform sampling. Thus, the weighted bandlimited interpolation is clearly the superior technique amongst four interpolation techniques considered here for the Doppler spectral estimation of nonuniform PRF waveforms.

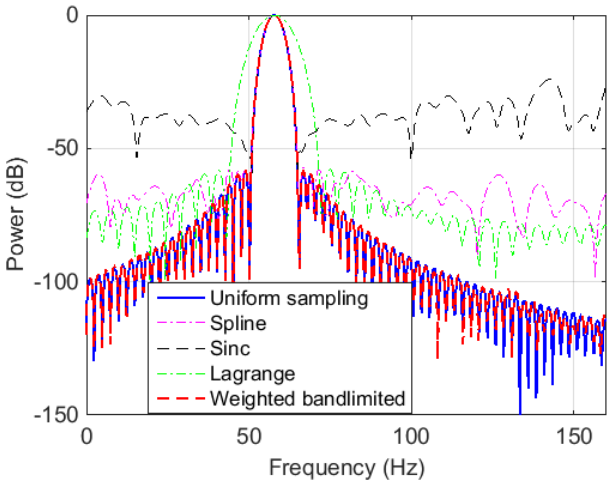

Fig. 2. Comparison of interpolation based spectral estimations of nonuniform sampled signals.

B. Detection in clutter

The iterative adaptive periodogram performs well amongst periodogram based or direct approaches, and the weighted bandlimited interpolation was found to be superior amongst interpolation techniques. Therefore, we choose these two techniques for further analysis. In this Section, we compare these two techniques considering the scenario of detecting low signal-to-clutter ratio (SCR) targets. The clutter was simulated by a summation of 500 complex exponentials randomly distributed in the frequency band $[-5.8, 16.7]$ Hz. Each clutter return has a random phase and a Gaussian distributed amplitude. Non-fluctuating (Swerling 0) target is present at 35.8 Hz. SCR is set to -51.8 dB. Doppler spectra obtained using different techniques for nonuniform PRF sampling with $\kappa = 0.3$ is shown in Figure 3.

The weighted bandlimited interpolation technique gives an Doppler spectrum which is almost identical to the uniformly sampled spectrum. The iterative adaptive periodogram gives a finer resolution (a minimal mainlobe width which is due to the non-application of the window), but at a higher computational cost. Though the iterative adaptive periodogram is a nonparametric model and does not strictly require a finite number of sinusoidal components in the signal analysed, the method performs most satisfactory when this condition is met [5]. In this spread Doppler clutter scenario the iterative approach is computationally costly, requiring up to 165 iterations and taking 17.26 s[1] to run in Matlab. On the other hand, the weighted bandlimited interpolation based approach only took 0.14 s to run. As expected, direct DFT on nonuniform samples is not capable of detecting a target in the presence of clutter.

Next, we analyse the Doppler response of a Swerling 2 target where target radar cross section (RCS) varies exponentially and decorrelates from pulse to pulse. This scenario can be used to assess the performance of the algorithms for non-

[1]Computation times are only mentioned for rough comparison purposes.

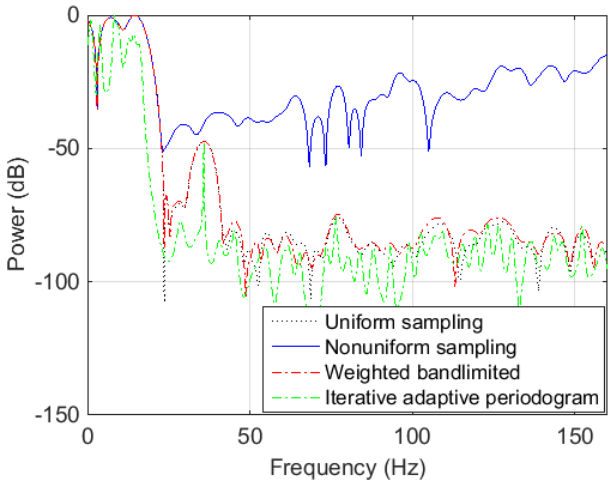

Fig. 3. Doppler spectra of nonuniform sampled signal in the presence of clutter for a non-fluctuating target.

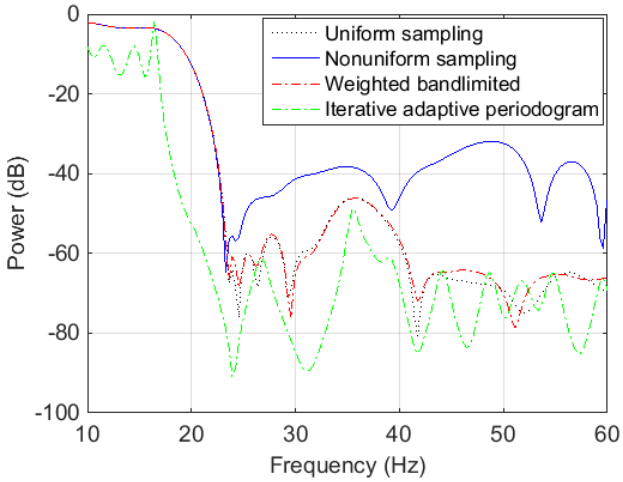

Fig. 4. Doppler spectra of nonuniform sampled signal in the presence of clutter for a Swerling 2 target.

pure sinusoidal returns which will always be the case with real data. Zoomed-in results for the frequency range of interest are shown in Figure 4. Again, the weighted bandlimited interpolation based technique gives an Doppler spectrum very similar to the uniform sampling case.

C. Discussion

The iterative adaptive periodogram achieves good Doppler resolution and clutter isolation, but its high complexity may hinder its usage in real-time applications. Nevertheless, this technique can be useful in Doppler processing of nonuniform PRF waveforms in non-time critical applications. We observe that noise floor is spikier in the iterative adaptive periodogram compared to the weighted bandlimited interpolation due to non-usage of a window. This may create more false alarms, or else the threshold needs to be increased for the same false alarm rate. Thus, even though the iterative adaptive periodogram has a sharper peak at the target Doppler, it may not necessarily translate into a better detection. A comprehensive probability of detection (P_d) *vs* probability of false alarms (P_{fa}) analysis is warranted to compare the two techniques, which is beyond the scope of this paper.

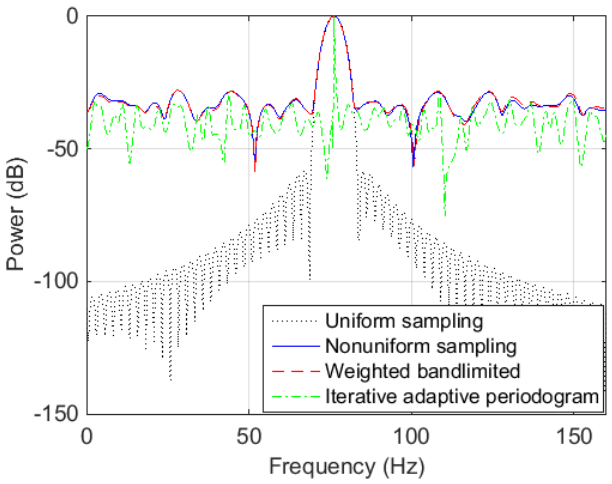

Fig. 5. Doppler aliased spectra of nonuniform sampled signal.

A major limitation in all the bandlimited and periodogram based techniques occurs when target's Doppler falls into a frequency outside the band determined by the PRF, i.e. Doppler aliased targets. In the weighted bandlimited interpolation, the weighting matrix $\mathbf{W}$ (13) is computed assuming that the signals of interest fall within B. For a signal where this assumption is not held, the accuracy of the spectrum will not be improved by $\mathbf{W}$. Hence, we observe a spectrum similar to direct DFT of nonuniform sampled data as shown in Figure 5. The iterative adaptive periodogram also degrades in this scenario as the basis $\mathbf{A}$ (5) does not capture the signals present. On the other hand, uniform sampling achieves the same sidelobes as in the non-aliased case, and true target Doppler may be solved using information available in the tracker. In all nonuniform sampling cases, the sidelobe levels have been increased up to -28 dB as opposed to -58 dB in the uniform sampling.

V. Conclusion

A number of methods based on periodogram and interpolation techniques have been presented for the sidelobe suppression of nonuniform PRF radar returns. The iterative adaptive periodogram and the weighted bandlimited interpolation techniques achieved desired sidelobe levels, although the iterative adaptive periodogram is computationally more complex. Limitations of the techniques were discussed. These techniques can be utilised for Doppler processing of nonuniform PRF waveforms which has many useful radar applications.

ACKNOWLEDGMENT

This work was done while the first author was on a short-term posting in the High Frequency Radar branch.

REFERENCES

[1] J. D. Scargle, "Studies in astronomical time series analysis. II-Statistical aspects of spectral analysis of unevenly spaced data," *The Astrophysical Journal*, vol. 263, pp. 835–853, 1982.

[2] R. Barbieri, E. C. Matten, A. A. Alabi, and E. N. Brown, "A point-process model of human heartbeat intervals: new definitions of heart rate and heart rate variability," *American Journal of Physiology-Heart and Circulatory Physiology*, vol. 288, no. 1, pp. H424–H435, 2005.

[3] R. McAulay, "The effect of staggered PRF's on MTI signal detection," *IEEE Transactions on Aerospace and Electronic Systems*, no. 4, pp. 615–618, 1973.

[4] N. R. Lomb, "Least-squares frequency analysis of unequally spaced data," *Astrophysics and space science*, vol. 39, no. 2, pp. 447–462, 1976.

[5] P. Stoica, J. Li, and H. He, "Spectral analysis of nonuniformly sampled data: A new approach versus the periodogram," *IEEE Transactions on Signal Processing*, vol. 57, no. 3, pp. 843–858, 2009.

[6] S. A. Dyer and J. S. Dyer, "Cubic-spline interpolation: Part 1," *IEEE Instrumentation & Measurement Magazine*, vol. 4, no. 1, pp. 44–46, 2001.

[7] C. E. Shannon, "Communication in the presence of noise," *Proceedings of the IRE*, vol. 37, no. 1, pp. 10–21, 1949.

[8] K. Yao and J. Thomas, "On some stability and interpolatory properties of nonuniform sampling expansions," *IEEE Transactions on Circuit Theory*, vol. 14, no. 4, pp. 404–408, 1967.

[9] L. C. Potter and K. Arun, "Energy concentration in band-limited extrapolation," *IEEE Transactions on Acoustics, Speech, and Signal Processing*, vol. 37, no. 7, pp. 1027–1041, 1989.

[10] M. Unser, "Sampling-50 years after Shannon," *Proceedings of the IEEE*, vol. 88, no. 4, pp. 569–587, 2000.

[11] A. Dutt and V. Rokhlin, "Fast Fourier transforms for nonequispaced data," *SIAM Journal on Scientific computing*, vol. 14, no. 6, pp. 1368–1393, 1993.

[12] P. Babu and P. Stoica, "Spectral analysis of nonuniformly sampled data–a review," *Digital Signal Processing*, vol. 20, no. 2, pp. 359–378, 2010.

[13] K. Yao and J. B. Thomas, "On truncation error bounds for sampling representations of band-limited signals," *IEEE Transactions on Aerospace and Electronic Systems*, no. 6, pp. 640–647, 1966.

[14] J.-P. Berrut and L. N. Trefethen, "Barycentric Lagrange interpolation," *SIAM review*, vol. 46, no. 3, pp. 501–517, 2004.